A new magnetic compass calibration algorithm using neural networks

Article *in* Measurement Science and Technology · December 2005

DOI: 10.1088/0957-0233/17/1/025

CITATIONS
61

READS
7,379

2 authors:

Jau-Hsiung Wang
Trimble Navigation
14 PUBLICATIONS **289** CITATIONS
SEE PROFILE

Yang Gao
The University of Calgary
260 PUBLICATIONS **5,840** CITATIONS
SEE PROFILE

INSTITUTE OF PHYSICS PUBLISHING MEASUREMENT SCIENCE AND TECHNOLOGY

Meas. Sci. Technol. **17** (2006) 153–160 doi:10.1088/0957-0233/17/1/025

A new magnetic compass calibration algorithm using neural networks

Jau-Hsiung Wang and Yang Gao

Department of Geomatics Engineering, The University of Calgary, Calgary, Alberta T2N 1N4, Canada

E-mail: gao@geomatics.ucalgary.ca

Received 13 July 2005, in final form 13 November 2005
Published 15 December 2005
Online at stacks.iop.org/MST/17/153

Abstract

The magnetic compass can provide heading direction by measuring the Earth's magnetic field. In practical applications, there usually exists an unwanted local magnetic field that will distort the magnetometer measurements; hence a calibration procedure is essential. Current calibration methods are limited by the inaccurate magnetometer error estimation when measurements are deteriorated by magnetic disturbances or large noises. This paper proposes a new compass calibration algorithm via modelling the nonlinear relationship between the compass heading and the true heading using neural networks. When an external heading reference is available, neural networks can be trained to properly model this nonlinear input–output pattern even in the presence of magnetic disturbances, and subsequently can be applied to convert the compass heading into the correct heading. The proposed algorithm does not require declination information and magnetometer biases and scale factor estimation. The simulation and field test results have verified the effectiveness and robustness of the proposed calibration method and have also shown that the calibration performance is proportional to the quality of the training data.

Keywords: magnetometer, heading, calibration, neural networks

(Some figures in this article are in colour only in the electronic version)

1. Introduction

The magnetic compass has been widely used for heading determination in pedestrian and vehicular navigation. It can be integrated with gyros to remove gyro drift errors and to provide more reliable heading information (Ladetto *et al* 2001a, Wang and Gao 2004). With known object speed or distance travelled, a magnetic compass can provide dead-reckoning navigation to help a GPS-based navigation system during the loss of GPS signals (Ladetto *et al* 2001b, Wang and Gao 2005). A modern magnetic compass consists of a triad of magnetometers mounted orthogonally in a vehicle to measure the strength of the Earth's magnetic field vector in body coordinates. With tilt information, the measured magnetic field vector can be projected onto the Earth's surface to determine the angle between the longitudinal axis of a vehicle and magnetic north. Then, by adding or subtracting a proper declination angle to correct for true north, the vehicle heading can be determined. In reality, however, the Earth's magnetic field is usually distorted by unwanted local magnetic fields contributed by nearby ferrous effects and external interference. To obtain a correct vehicle heading using a magnetic compass, the process of calibrating magnetometer measurements is essential.

Two types of methods, one requiring a reference heading, another not, have been successfully used for compass calibration. When a reference heading is unavailable, a simple calibration method is to level and rotate the compass on a horizontal surface and to find the maximum and minimum values of the x and y axes magnetic readings. Then these four values can be used to compute the magnetometer scale factors and biases based on the fact that the locus of error-free measurement on the x and y axes is a circle (Caruso 1997). Another similar method developed by Gebre-Egziabher *et al* (2001) is to use a nonlinear two-step estimator to resolve an ellipse locus equation and then to estimate the scale factors and biases. In addition, Crassidis *et al* (2005) developed a

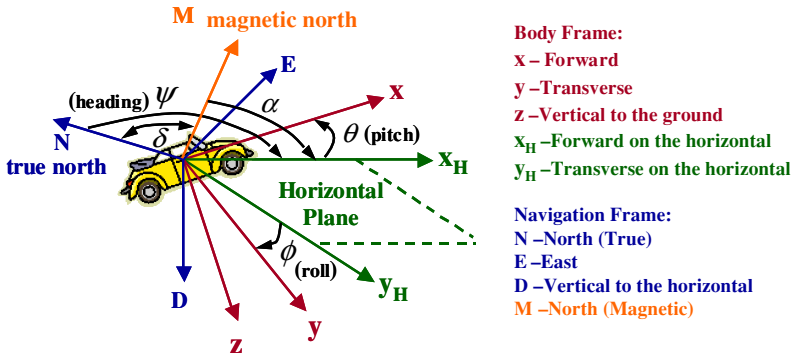

Figure 1. Heading determination using three-axis magnetometers.

real-time approach for compass calibration using an extended Kalman filter and an unscented filter. This approach relies on a conversion of the magnetometer-body and geomagnetic-reference vectors into an attitude-independent observation by using scalar checking (Crassidis *et al* 2005). On the other hand, if a reference heading is known during the calibration process, a traditional 'swinging' procedure involving levelling and rotating the compass through a series of known headings can be used (Bowditch 1995). At each known heading, the heading error is computed and these known headings and heading errors will be used to estimate the unknown parameters in the heading error equation using a batch least-squares estimation. Once the parameters are solved correctly, the heading error can be predicted based on the heading error equation as a nonlinear input–output mapping. However, the common drawback of the aforementioned calibration methods is that the algorithm will diverge or fail while the measurements are deteriorated by large amounts of noise and/or blunders. This prohibits compass calibration from many practical applications.

This paper proposes a new compass calibration algorithm by applying neural networks nonlinear mapping between the compass heading and true heading based on the fact that the incorrect heading estimates due to the magnetometer biases, scale factors and declination angles have a nonlinear relationship with the true heading. When an external heading reference is available, neural networks are trained to model this nonlinear relationship. After that, the trained neural networks can be used to convert the compass heading into the correct heading. By properly selecting the architecture of the network and the size of the training data set, neural networks can ignore spurious disturbances and will produce a correct input–output mapping (Haykin 1999), making the proposed calibration algorithm more robust in practical applications where magnetic disturbances and tilt compensation errors exist. In the rest of this paper, the principle of magnetic compassing and the errors affecting compass heading will be discussed first. Then the design of neural networks for compass heading calibration will be presented. Several simulation and field tests will be presented to assess the performance of the proposed method.

2. Magnetic compass error model

The principle of magnetic compassing is to measure the Earth's magnetic field that has a component parallel to the Earth surface that always points towards the magnetic north. Because the magnetometers attached to a moving vehicle are most often not confined to the Earth's surface, it is essential to use three-axis magnetometers mounted orthogonally so that the Earth's magnetic field can be fully rotated back to a horizontal orientation as shown in figure 1. The magnetic compass is aligned with the body frame consisting of three orthogonal axes where x is in the direction of forward motion of the vehicle, z is in the downward direction to the road surface and y is in the direction of transverse motion of the vehicle, perpendicular to the plane formed by the x and z axes. The attitude of the vehicle is represented by three Euler angles, roll (ϕ), pitch (θ) and heading (ψ), which are the rotation angles about the x, y and z axes, respectively. With the knowledge of tilt (pitch and roll) angles, the measured magnetic field vector can be projected on a horizontal plane parallel to the Earth's surface in the following manner (Caruso 1997):

$$\begin{bmatrix} M_{x\mathrm{H}} \\ M_{y\mathrm{H}} \end{bmatrix} = \begin{bmatrix} \cos\theta & \sin\theta\sin\phi & -\cos\phi\sin\theta \\ 0 & \cos\phi & \sin\phi \end{bmatrix} \begin{bmatrix} M_x \\ M_y \\ M_z \end{bmatrix}, \quad (1)$$

where M_x, M_y and M_z are the magnetometer measurements of the body frame. $M_{x\mathrm{H}}$ and $M_{y\mathrm{H}}$ are the magnetometer measurements of the body frame projected on the horizontal plane formed by the x_{H} and y_{H} axes.

Then the angle α between the forward axis of the vehicle and magnetic north can be calculated by resolving the horizontal component of the magnetometer measurements as shown in equation (2)

$$\alpha = \begin{cases} 90, M_{x\mathrm{H}} = 0, M_{y\mathrm{H}} < 0 \\ 270, M_{x\mathrm{H}} = 0, M_{y\mathrm{H}} > 0 \\ 180 - \arctan\left(\dfrac{M_{y\mathrm{H}}}{M_{x\mathrm{H}}}\right) \times \dfrac{180}{\pi}, M_{x\mathrm{H}} < 0 \\ -\arctan\left(\dfrac{M_{y\mathrm{H}}}{M_{x\mathrm{H}}}\right) \times \dfrac{180}{\pi}, M_{x\mathrm{H}} > 0, M_{y\mathrm{H}} < 0 \\ 360 - \arctan\left(\dfrac{M_{y\mathrm{H}}}{M_{x\mathrm{H}}}\right) \times \dfrac{180}{\pi}, M_{x\mathrm{H}} > 0, M_{y\mathrm{H}} > 0. \end{cases} \quad (2)$$

Finally, by adding or subtracting the proper declination angle δ to correct for true north, the vehicle heading ψ can be determined. The declination angle can differ by $\pm 25^\circ$ or more and can be determined from a lookup table based on the geographic location. But it should be noted that the declination angle will change secularly according to the variations of the Earth's geomagnetic field (Whitcomb 1989).

In most practical applications, the magnetic compass is mounted in vehicles and on platforms where unwanted local magnetic fields exist. These unwanted local magnetic fields caused by nearby ferrous effects such as steel materials and external interference such as dc current will distort or bend the Earth's magnetic field and result in incorrect compass heading determination. If the compass is securely mounted in a vehicle, the nearby ferrous effects on magnetometer measurements will remain stable and can be modelled as biases and scale factor errors on the measurements. However, external interference is the result of magnetic disturbances and will change over time randomly. Therefore, the magnetometer measurement error from external interference cannot be modelled. Further filtering is therefore often necessary to reduce this error. In addition to these environmental magnetic effects, the magnetometer triad may not be mounted in perfect alignment with the body frame and hence cross coupling of the magnetic field axes will result in magnetometer measurement errors. But compared to nearby ferrous effects, in general, the misalignment errors are much smaller and can be ignored. Thus, in most applications only biases and scale factor errors are dealt with by compass calibration. The magnetometer measurements in a horizontal plane can be modelled as

$$\hat{M}_{x\mathrm{H}} = \mathrm{SF}_{x\mathrm{H}} \times M_{x\mathrm{H}} + B_{x\mathrm{H}}, \tag{3}$$

$$\hat{M}_{y\mathrm{H}} = \mathrm{SF}_{y\mathrm{H}} \times M_{y\mathrm{H}} + B_{y\mathrm{H}}, \tag{4}$$

where $\hat{M}_{x\mathrm{H}}$ and $\hat{M}_{y\mathrm{H}}$ are the actual values of the Earth's magnetic field projection on the horizontal plane. $\mathrm{SF}_{x\mathrm{H}}$, $\mathrm{SF}_{y\mathrm{H}}$, $B_{x\mathrm{H}}$ and $B_{y\mathrm{H}}$ are the scale factors and biases of the magnetometer measurements on x_{H} and y_{H} axes, respectively.

Thus, in accordance with the magnetometer error model and the heading computation equation, the combination of biases, scalar factors and declination angles will result in an incorrect heading estimate that has a nonlinear relationship with the true heading.

3. Magnetic compass calibration using neural networks

As mentioned previously, most compass calibration methods estimate the magnetometer biases and scale factors based on the heading error model or the ellipse locus equation. The bias and scale factor estimates, however, would be inaccurate if the magnetometer measurements during the estimation process are deteriorated by external disturbances with large noise or non-Gaussian errors. To overcome this problem, we propose a new method for compass calibration using neural network nonlinear mapping. Unlike the calibration algorithms presented before, this algorithm does not estimate the magnetometer biases and scale factors and does not need to know the declination angles for the heading correction for true north. The proposed calibration algorithm is based on the fact that the incorrect heading estimate due to the magnetometer biases, scale factors and declination angles has a nonlinear relationship with the true heading. Shown in figure 2 are some examples of such a nonlinear relationship for a two-axis compass in a horizontal plane. The added biases on each axis are from -0.4 to 0.4 times the horizontal magnitude of the reference magnetic field, scale factors from 1 to 1.5 and declination angles from -20 to 20°. It can be seen that this

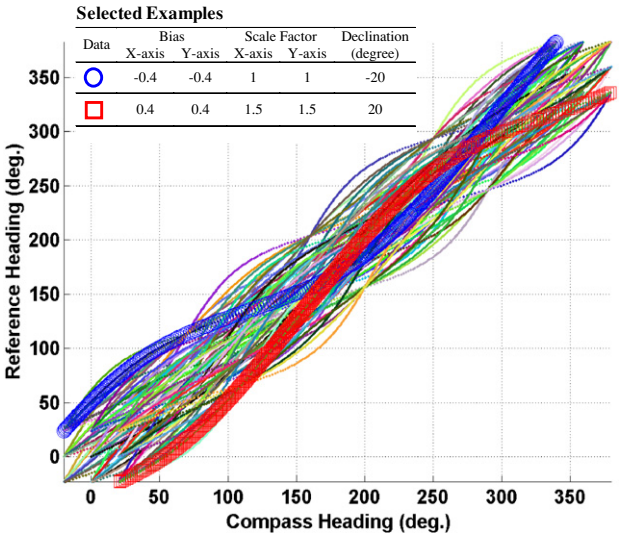

Figure 2. Nonlinear relationship between compass heading and true heading.

nonlinear relationship describing the effects of biases, scale factors and declination angles in heading domain can be used for compass heading calibration.

In this research, we apply artificial neural networks to model this nonlinear mapping between the compass heading and true heading because of the following advantages (Haykin 1999).

(1) Nonparametric statistical inference: neural networks can provide a model-free input–output nonlinear mapping that does not require a prior statistical model for the input data.
(2) Generalization: neural networks can produce reasonable outputs for inputs not encountered during training (learning).
(3) Nonstationary environment operation: neural networks that have been trained to operate in a specific environment can be retrained to deal with minor changes in the operating environmental conditions.

The input and output of the neural networks are compass heading and true heading. Neural networks are trained to model the input–output pattern when true headings are available. In most applications since the compass is a supplementary heading sensor for the GPS or GPS/INS navigation system, the true heading can be provided by GPS or GPS/INS integration when GPS signals are available. When the compass becomes the primary sensor for heading determination, the trained neural networks are used to correct the compass heading. If the magnetometer errors or the operating environmental conditions change from the training data, neural networks can be retrained to adapt to the up-to-date input–output relationship. By properly selecting the principal time constants of the mapping system, neural networks can ignore spurious disturbances and respond to meaningful changes in the environment. This is a very important feature of neural networks for dealing with magnetic disturbances during the training/learning process.

As shown in figure 3, multi-layer feed-forward neural networks are used in this paper for mapping compass heading into true heading. The input layer accepts the input signal and

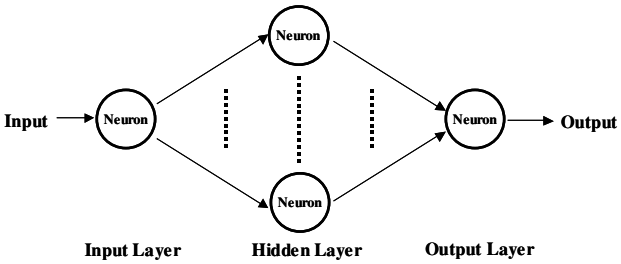

Figure 3. Example of multi-layer feed-forward neural networks.

distributes it to the next layer. The neurons in the next layer pass the net input to an activation function that calculates the output for each node. This procedure is repeated for each layer until the output layer.

Denote the synaptic weight between the ith neuron in the $(k-1)$th layer and the jth neuron in the kth layer as $W_{ji}^{(k-1)}$, and the output, activation function and the threshold of the jth neuron in the kth layer as $y_j^{(k)}$, $f_j^{(k)}(.)$ and $\theta_j^{(k)}$, respectively. If the number of neurons in the kth layer is N_k and the number of layers including the input and output layer is M, the input–output relationship for each neuron can be described as

$$y_j^{(k)} = f_j^{(k)}\left(\sum_{i=1}^{N_{k-1}} W_{ji}^{(k-1)} y_i^{(k-1)} - \theta_j^{(k)}\right), \tag{5}$$

where $j = 1, 2, \ldots, N_k;\ k = 1, 2, \ldots, M$.

In this paper, a nonlinear sigmoid (logsig) activation function defined in the following is utilized to provide the nonlinearities. This activation function is commonly used in back-propagation networks, in part because it is differentiable

$$f(v) = \frac{1}{1 + \mathrm{e}^{-\beta v}}, \tag{6}$$

where β is the slope parameter.

Thus, the outputs of the network, $y_1^{(M)}, y_2^{(M)}, \ldots, y_{N_M}^{(M)}$, are nonlinear combinations of network inputs, all of the prior neurons' outputs and parameters.

A back-propagation training/learning algorithm is then utilized to modify the synaptic weights of the networks by minimizing the difference between the desired response and the actual response of the networks produced by the input signal in accordance with an appropriate statistical criterion. This algorithm consists of two passes through different layers of the network: a forward pass and a backward pass. In the forward pass, the synaptic weights of the networks are all fixed and a set of outputs is produced forward through the networks as the actual response of the networks based on equation (5). During the backward pass, the synaptic weights of the networks are all adjusted backward through the networks in accordance with an error-correction rule seeking a direction for weight change that reduces the value of the cost function. The training of the networks is repeated for many examples in the set until the networks reach a steady state so that a proper input–output mapping is constructed. It should be noted that the number of neurons and the layers used will affect the performance of the input–output mapping. In general, the optimal architecture is empirically chosen based on the physical complexity of the problem at hand. In this study, three-layer neural networks with 12 neurons in the hidden layer are used for the nonlinear mapping between compass heading and true heading. More detailed information about the foundation of neural networks may be found in Haykin (1999).

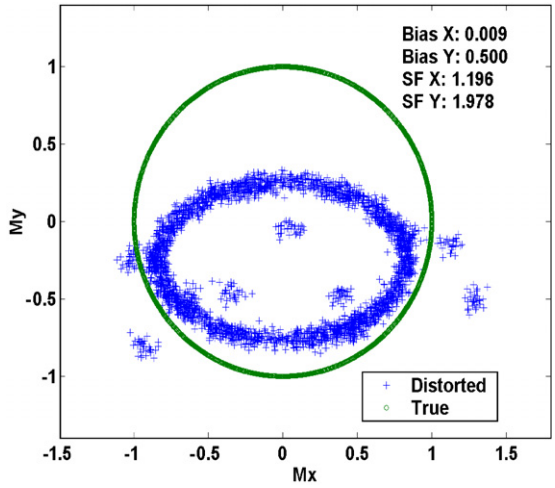

Figure 4. Magnetic field measurement locus in 2D.

4. Simulation studies

In this section, the performance using neural networks for the nonlinear mapping between compass heading and true heading is examined by simulation data. Two-dimensional magnetic fields covering 360° direction in the horizontal plane are generated as the reference data. The magnetometer biases, scale factors, noise and disturbances are added to the reference data to produce the distorted magnetometer measurements. The compass heading is then computed using the distorted magnetometer measurements and biased by a selected declination angle. Figure 4 shows an example of the true and distorted magnetic field measurement loci in 2D. In this simulation data set, the added biases on the x and y axes are randomly selected as 0.009 and 0.5 times the horizontal magnitude of the reference magnetic field, while the scale factors on the x and y axes are 1.196 and 1.978, respectively. Gaussian white sequences with a standard deviation of 3.5% of the horizontal magnitude of the reference magnetic field are also added as noise effects. The magnetic disturbances are simulated as biasing the magnetic field measurements with a randomly selected magnitude smaller than 60% of the horizontal magnitude of the reference magnetic field. Twelve randomly selected data sets, evenly spreading over the entire reference data and accounting for 12.5% of the total reference data, are deteriorated by simulated disturbances. Figure 5 shows the performance using neural networks for nonlinear mapping between the reference heading and the distorted compass heading biased by a randomly selected declination angle of −9.59°. The blue cross markers represent the training data set and the green circle markers are the neural network outputs from the processing of the disturbance-free testing data that have the same biases, scalar factors and declination angles as the training data. It can be seen that even the training data are deteriorated by noise and disturbances, neural networks have modelled the nonlinear relationship between the reference heading and compass heading properly.

Table 1. Statistical analysis of calibrated heading accuracy (12.5% data deteriorated by disturbances).

	Sensor error				Calibrated heading error		
Test no.	Bias-x	Bias-y	SF-x	SF-y	Declination (deg)	Mean (deg)	RMS (deg)
1	0.223	0.162	1.393	1.592	7.998	−0.621	2.059
2	0.13	−0.153	1.699	1.397	−7.777	−0.264	1.456
3	−0.478	−0.305	1.791	1.815	19.333	0.245	2.196
4	0.203	−0.005	1.565	1.767	5.964	0.672	2.827
5	−0.139	0.596	1.982	1.9	−4.725	−0.909	2.149
6	−0.331	−0.136	1.162	1.031	15.189	−0.94	3.503
7	0.009	0.5	1.196	1.978	−9.594	−0.252	2.777
8	0.297	0.175	1.743	1.651	5.419	−0.45	1.458
9	0.155	−0.248	1.168	1.814	9.688	0.904	2.466
10	−0.019	0.492	1.735	1.005	−20.873	−0.148	2.615

Table 2. Statistical analysis of calibrated heading accuracy (6.25% data deteriorated by disturbances).

	Sensor error				Calibrated heading error		
Test no.	Bias-x	Bias-y	SF-x	SF-y	Declination (deg)	Mean (deg)	RMS (deg)
1	−0.476	0.352	1.874	1.237	−20.44	1.059	2.673
2	0.193	−0.223	1.217	1.231	−5.706	0.713	1.156
3	−0.574	−0.189	1.727	1.489	−20.244	0.176	2.962
4	−0.038	−0.445	1.584	1.603	−6.591	0.211	1.9
5	0.109	−0.491	1.401	1.191	2.438	−0.501	1.162
6	0.276	−0.522	1.221	1.19	3.755	0.371	1.289
7	0.189	0.098	1.119	1.519	0.676	−0.027	2.986
8	−0.571	−0.022	1.543	1.379	3.928	−0.48	2.487
9	0.191	0.22	1.364	1.616	4.956	0.324	1.18
10	0.198	0.08	1.099	1.681	22.912	0.512	1.279

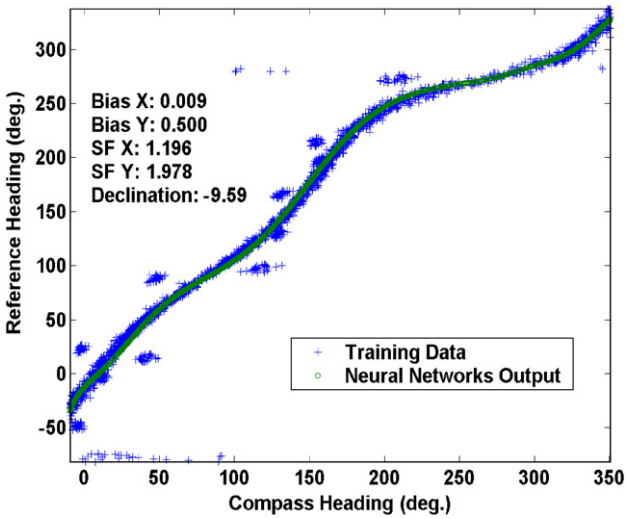

Figure 5. Performance of neural network nonlinear mapping.

It should be noted that the compass calibration is only used for removing the heading errors caused by biases, scalar factors and declination angles. Measurement noise and magnetic disturbances could be reduced by further filtering or integration with additional sensors.

To assess the performance of the neural network nonlinear mapping statistically, more simulation tests have been performed. The simulation results are summarized in table 1. In each simulation, the biases, scalar factors and declination angles are randomly selected. Noise and disturbances are then added in the same manner as described before to form the training data. After the training process, the neural networks process the disturbance-free testing data that have the same biases, scalar factors and declination angles as the training data and output the calibrated heading. Then the calibrated heading error is computed by taking the difference between the neural network output and the true heading. The average mean and RMS values of the calibrated heading errors in these ten simulation tests are equal to -0.176° and 2.35°, respectively. This shows the capability of training neural networks for nonlinear input–output mapping in the presence of magnetic disturbances.

To further study the effect of magnetic disturbances on the performance of the neural network-based compass calibration, we have also performed additional simulation tests with the data deteriorated by different levels of disturbances. Tables 2 and 3 summarize the simulation results while 6.25% and 25% of training data are deteriorated by disturbances, respectively. The average mean and RMS values of the calibrated heading errors are -0.236° and 1.907° for table 2 and -0.855° and 4.373° for table 3. It can be seen that the performance of the neural network-based compass calibration will degrade with increased data deterioration by disturbances. The results also demonstrate that the proposed calibration algorithm is still able to work under certain interference environments, e.g. 25% data deteriorated by disturbances, while other calibration algorithms have failed in bias and scalar factor estimation. This shows the robustness of the proposed neural network-based compass calibration algorithm.

5. Experimental results

A further verification of the proposed compass calibration algorithm was carried out in field tests with a low-cost MEMS

Table 3. Statistical analysis of calibrated heading accuracy (25% data deteriorated by disturbances).

	Sensor error				Calibrated heading error		
Test no.	Bias-x	Bias-y	SF-x	SF-y	Declination (deg)	Mean (deg)	RMS (deg)
1	0.213	−0.281	1.411	1.4	−19.832	0.336	4.137
2	0.035	0.421	1.136	1.532	3.132	−2.476	4.437
3	−0.244	−0.099	1.509	1.074	2.09	2.327	4.574
4	−0.016	−0.091	1.287	1.893	−6.269	0.001	4.105
5	−0.463	−0.555	1.77	1.368	−19.414	−2.51	6.216
6	−0.163	−0.517	1.461	1.513	−11.922	−2.538	3.553
7	−0.19	0.598	1.982	1.412	3.95	−0.569	2.94
8	−0.544	−0.257	1.647	1.447	23.494	−0.911	4.62
9	−0.078	−0.268	1.24	1.49	−11.57	−1.471	5.241
10	−0.153	−0.037	1.989	1.303	−13.005	−0.737	3.909

Table 4. MT9 specifications.

Parameter	Gyro (deg s^{-1})	Accelerometer (m s^{-2})	Magnetometer (mG)
Operating range	±900	±20	±750
Linearity	0.1	0.2	1
Bias stability (1σ)	5	0.02	0.5
Noise (RMS)	0.7	0.01	4.5

inertial sensor, namely MT9 made by Xsens Inc., mounted in a van where unwanted local magnetic fields due to steel structure and dc current exist. The MT9 contains a three-axis gyro, a three-axis accelerometer and a three-axis magnetometer with the sensor specifications shown in table 4. A tactical grade Honeywell HG1700 IMU and a NovAtel OEM-4 GPS receiver have been used to provide geo-referencing solutions. The reference attitude, velocity and position information were provided by the P3-INS software package developed by the Positioning and Mobile Information Systems Group (PMIS) in the Department of Geomatics Engineering at the University of Calgary. The P3-INS can be considered as a next generation position and attitude determination system via integration of precise point positioning (PPP) and inertial technologies since the traditional GPS reference stations are no longer required. It determines position and attitude based on the integration of inertial data and undifferenced observations from a single GPS receiver. It can provide globally attainable accuracy for position at the centimetre to decimetre level and for attitude at the several arcmin level (Zhang and Gao 2005).

The field test was performed in a parking lot at the University of Calgary. The data output rate was 20 Hz. First, we drove the test van along a rectangular trajectory to collect a certain number of magnetometer measurements as shown in figure 6. It can be seen that the Earth's magnetic fields had been biased, distorted and interfered by the local magnetic fields inside a typical land vehicle. These deteriorated magnetic measurements were first rotated back to a horizontal orientation with the tilt angles provided by MEMS inertial sensors and then used to calculate the compass heading. The true heading provided by GPS/gyro integration using the Kalman filter was synchronized with the compass heading to form the training data. It should be noted that the accuracy of the compass heading is also affected by tilt errors.

Figure 7 shows the training data set and the trained neural network outputs from the processing of the same data set. It can be seen that the nonlinear input–output relationship has been modelled properly even though the training data were deteriorated by noise, magnetic disturbances and tilt compensation errors. However, there exist modelling errors resulting from the insufficient and imperfect training data. Proper determination of the size of the training data set needed

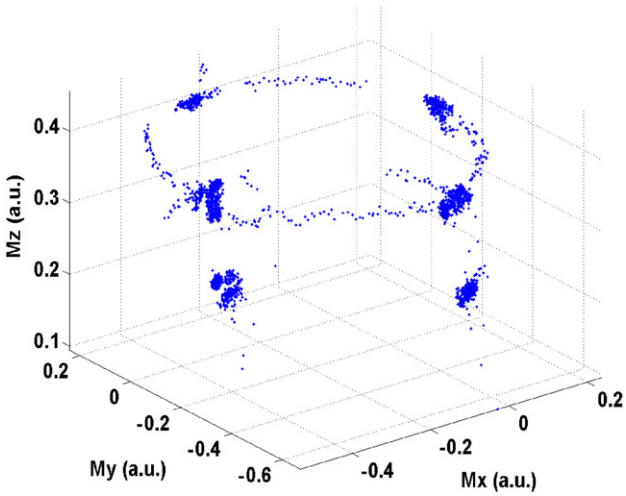

Figure 6. Measured magnetic field for neural network training.

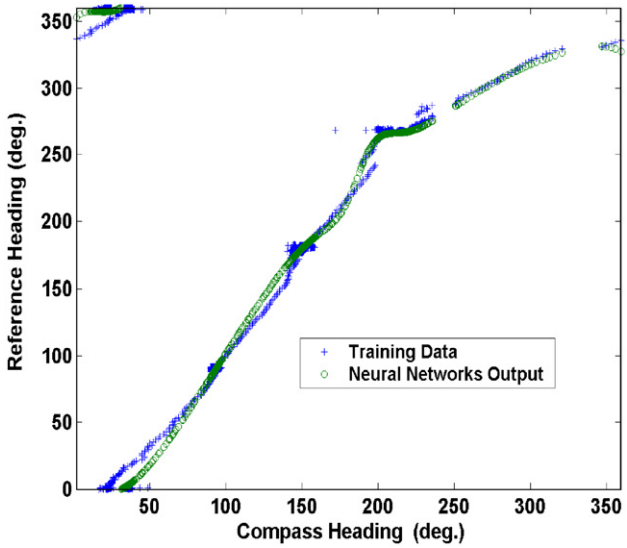

Figure 7. Neural network training result.

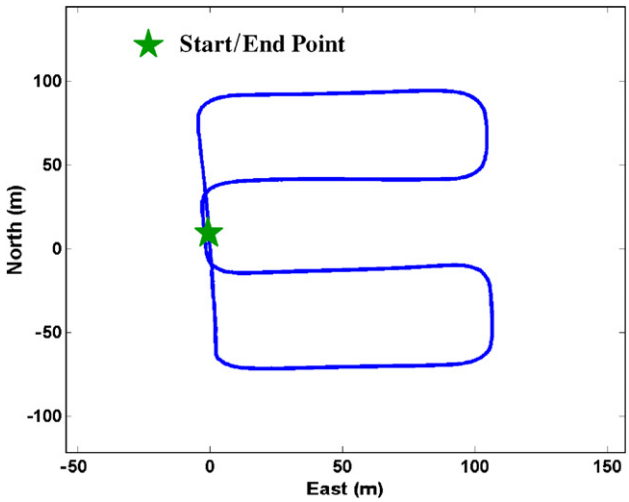

Figure 8. Test trajectory.

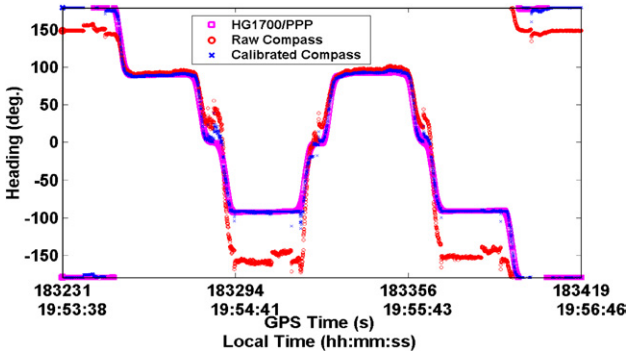

Figure 9. Pre- and post-calibration heading.

for more accurate input–output mapping is another practical issue and is a subject for further studies.

After the training process, we drove the van along a different trajectory as shown in figure 8 to examine the performance of the proposed calibration algorithm. The compass headings before and after the calibration compared to the reference heading are shown in figure 9. In general, the compass heading has been calibrated close to the reference heading, which confirms the effectiveness of the proposed calibration algorithm. However, the jump errors resulting from magnetic disturbances and tilt compensation errors cannot be removed by compass calibration and should be reduced by further filtering such as using a low pass filter or integration with a gyroscope. For the purpose of statistical analysis, we repeated the test along the same route and calculated the heading error in each test as summarized in table 5. The average mean and RMS values of the calibrated heading errors are equal to -1.927 and 6.226° which are much larger than the simulation results. This is due to larger disturbances in the testing data since there exist certain disturbances in the field tests that are not present in the simulation tests. In summary, both simulation and field tests have verified that the proposed calibration algorithm can be carried out in the presence of magnetic disturbances. Increasing the size of the training data or using less deteriorated training data is expected to improve the calibration performance.

Table 5. Statistical analysis of calibrated heading accuracy (field test data in a land vehicle).

	Calibrated heading error	
Test no.	Mean (deg)	RMS (deg)
1	−1.997	6.389
2	−1.908	5.944
3	−1.8	6.505
4	−1.907	6.643
5	−1.939	6.479
6	−1.786	6.151
7	−2.069	6.444
8	−1.988	5.998
9	−2.039	6.064
10	−1.834	5.643
Average	−1.927	6.226

6. Conclusions

A new compass calibration algorithm has been developed based on modelling the nonlinear relationship between the compass heading and the true heading using neural networks. This calibration algorithm does not require declination information and magnetometer bias and scale factor estimation. In the presence of magnetic disturbances and non-Gaussian errors, this calibration algorithm can still be carried out for learning input–output mapping while other calibration methods may fail in the magnetometer error estimation. Both the simulation and field test results have shown that the proposed algorithm can calibrate the compass heading within an accuracy of several degrees while the calibration performance is proportional to the quality of the training data. Further research work includes intelligent determination of the size of the training data and the frequency of the training process in accordance with the actual field environments. It is also recommended to reduce the heading errors caused by magnetic disturbances and tilt compensation errors using filtering or sensor fusion.

Acknowledgments

This study was partially supported by the Natural Science and Engineering Research Council of Canada (NSERC) and the Network Centers of Excellence (NCE)'s Geomatics for Informed Decisions (GEOIDE) programme.

References

Bowditch N 1995 *The American Practical Navigator* (Bethesda, MD: Defense Mapping Agency, Hydrographic/ Topographic Center)

Caruso M J 1997 Application of magnetoresistive sensors in navigation systems *Sensors Actuators* **1220** 15–21

Crassidis J L, Lai K-L and Harman R R 2005 Real-time attitude-independent three-axis magnetometer calibration *J. Guid. Control Dyn.* **28** 115–20

Gebre-Egziabher D, Elkaim G H, Powell J D and Parkinson B W 2001 A non-linear, two-step estimation algorithm for calibrating solid-state strapdown magnetometers *Proc. Int. Conf. on Integrated Navigation Systems (St Petersburg, Russia, 28–30 May 2001)*

Haykin S 1999 *Neural Networks: A Comprehensive Foundation* (Upper Saddle River, NJ: Prentice-Hall)

Ladetto Q, Gabaglio V and Merminod B 2001a Two different approaches for augmented GPS pedestrian navigation *Int. Symp. on Location Based Services for Cellular Users (Munich, Germany, 5–7 Feb. 2001)*

Ladetto Q, Gabaglio V and Merminod B 2001b Combining gyroscopes, magnetic compass and GPS for pedestrian navigation *Int. Symp. on Kinematic Systems in Geodesy, Geomatics and Navigation (KIS) (Banff, Canada, 5–8 June 2001)*

Wang J-H and Gao Y 2004 Fuzzy logic expert rule-based multi-sensor data fusion for land vehicle attitude estimation *Proc. 19th Int. Committee on Data for Science and Technology (CODATA) Conf. (Berlin, Germany, 7–10 Nov. 2004)*

Wang J-H and Gao Y 2005 An intelligent MEMS IMU-based land vehicle navigation system enhanced by dynamics knowledge *Proc. US Institute of Navigation (ION) 61st Ann. Meeting (Cambridge, MA, 27–29 June 2005)*

Whitcomb L 1989 Sensor compensation for vehicle magnetic signature *IEEE Aerosp. Electron. Syst. Mag.* **4** 33–7

Zhang Y and Gao Y 2005 Performance analysis of a tightly coupled Kalman filter for the integration of undifferenced GPS and inertial data *Proc. US Institute of Navigation (ION) 2005 National Technical Meeting (San Diego, CA, 24–26 Jan.)*